Conference Proceedings

EuroSun 2016
Palma de Mallorca (Spain), 11 - 14 October 2016

Considerations for using a rotary kiln for high temperature industrial processes with and without thermal storage

Alessandro Gallo[1,2], María Isabel Roldán[3], Elisa Alonso[1] and Edward Fuentealba[1]

[1] University of Antofagasta. Centro de Desarrollo Energético de Antofagasta (Chile)

[2] Doctorado en "Ciencias Aplicadas al Medio Ambiente" (RD99/11). University of Almeria (Spain).

[3] Plataforma Solar de Almería, Centro de Investigaciones Tecnológicas, Energéticas y Medioambientales (Almería, Spain)

Abstract

In this work, technical considerations and a comprehensive discussion on solar rotary kilns are reported. Rotary kilns permit to obtain well-mixed particles in a broad range of temperatures (up to 2000°C), and, for this reason, they are widely used for treating solid particles in several industrial sectors. In solar research field, they have been employed for processing materials in solar furnaces and, in some cases, they have also been proposed as receivers in solar tower plants. The aim of this work is to investigate the potential of solar rotary kilns as thermal receivers in solar tower plants, taking into account the constraints that limit their use. In particular, because of the shape of these reactors, circular heliostat fields are not allowed and the maximum power of the receiver is limited to less than 100 MWth. Thus, the reference case of a 50-MW_{th} central tower plant for the heating of sand as heat transfer medium is reported. Residence time and receiver thermal efficiency are evaluated using an analytical method. In addition, two possible heliostat fields with different size of mirrors are also proposed.

Keywords:*Concentrating solar heat, rotary kilns, industrial applications, scaling-up, thermal storage*

1. Introduction

Fossil fuels are currently the main energy source for heat-demanding industrial processes. However, solar thermal technologies can replace them offering an environmentally friendly and widely available solution. Different solar thermal technologies operate at low, medium and high temperature and can be considered to provide heat for industrial processes of variable requirements (Calderoni et al., 2012; Fuller, 2011; Lauterbach et al., 2012). Concentrating systems employ reflectors in order to collect the solar beams on a small area where the power levels are intensified (Liu et al., 2016). With concentration ratios of around 1000, systems efficiencies are maximized at high temperatures (700-1500 ºC). This represents a relevant advantage concerning the use of concentrating solar heat to drive high-temperature industrial processes (Romero and Steinfeld, 2012). Some of the most studied applications of concentrating solar energy, apart from electricity generation, focus on the production of solar fuels, including hydrogen, which is based on H_2O/CO_2 splitting and decarbonization processes (cracking, reforming, and gasification of carbonaceous feedstock) (Steinfeld, 2005). Other industrial applications are extractive metallurgy, ceramic material processing and calcination (Halmann et al., 2012; Meier et al., 2004; Nikulshina et al., 2009).

Concentrating solar energy can be coupled with thermal energy storage (TES) systems, representing an important advantage with respect to other renewable energy technologies as photovoltaics and wind. In the last years, efforts have been focused on developing more efficient TES with higher storage capacity in order to make concentrating solar energy more cost effective. Molten salts able to storage sensible heat are currently the more commercially exploited TES system but many other solutions are also under development (Kousksou et al., 2014; Mahlia et al., 2014; Pardo et al., 2014). Concerning the present work, the solar heating of solid materials, normally in form of particles, has been previously used to storage the energy as sensible heat (Gallo et al., 2015; Jemmal et al., 2016; Zhang et al., 2016) or as a combination of sensible and thermochemical heat (Alonso et al., 2015; Aydin et al.,

doi:10.18086/eurosun.2016.02.04 Available at http://proceedings.ises.org

2015; Block and Schmücker, 2016).

Receptors/reactors design plays an important role for increasing the efficiency of high temperature processes driven by concentrated solar energy. In direct absorption devices, there is not opaque barrier between the radiation and the absorber material. This material is usually the one that have to be heated as the final purpose of the tested process, such as an industrial reactant or a storage material. Direct absorption particles in solar receivers or reactors are commonly employed where the objective is to increase the temperature of such particulate material. Different types of particles can be found in literature according its configuration and performance (Alonso and Romero, 2015). Some authors have tried to innovate and to design novel engineering concepts. Many others have readapted classical technologies to integrate the direct solar radiation.

Rotary kilns have a long history of use in metallurgical and chemical industries, their performance is well known and they are able to operate at a very wide range of high temperatures (up to 2000 ºC) with greater thermal efficiencies than other reactor types. Since it is a well-known technology, several authors have developed prototypes of solarized rotary kilns that have been successfully demonstrated for different applications (Alonso et al., 2015). This work tries to analyze some relevant aspects of applying such a technology for industrial processes. A preliminary design of a 50-MW_{th} plant coupled with a rotary receiver is presented. Particles of sand are considered to be heated up until 750 ºC. With this assumption, an estimation of the kiln dimensions, residence time and particles flow-mass is given. A heliostat field design is optimized in order to reduce optical losses on the receiver aperture. The possibilities for integrating thermal storage within the solar plant are also discussed in this work.

2. Methodology for the preliminary design

The proposed methodology for the scale up of a solar tower plant based on a rotary kiln as central receiver consists of three main parts. In the first part, a simplified sizing of the kiln was carried out. Calculations were based on kilns working in a continuous mass-flow mode. In the second part, in order to calculate the receiver efficiency and to predict the thermal load, a thermal model was developed. This model was applied to a rotary kiln for the heating of sand without a quartz window at the aperture. Finally, in the last part, two heliostat fields based on different heliostat sizes were designed for such a receiver.

2.1. Receiver sizing

2.1.1. Industrial rotary kiln

Rotary kilns are widely utilized for several industrial processes because they supply well-mixed particles. In this way, uniform temperatures are obtained in the products. These reactors can be considered as a sort of cylindrical heat exchanger in which a gas phase transfers the heat to a solid phase. Generally, rotary kilns operate in continuous mode. In this system, particles are introduced at one of the ends and are extracted at the other one. The kiln usually presents a slight slop s to favor the particles axial movement. In the radial directions, particles movement depends mainly on both the rotational speed N and the Fill Ratio FR (percentage of reactor volume occupied by the particles). Different “bed-motions”, which depend on the kind of particles (size, shape, density) and wall-particle friction coefficient, can be achieved. Usually, rolling and cascading modes are the most used behaviors for industrial applications. The residence time τ is a measure of the particle permanence inside the reactor and it depends only on geometrical and operation parameters. Differently, a solar rotary reactor presents an aperture at one end of the kiln. In this way, the solar radiation can enter inside the device and impinges directly on solid particles. In some cases, a transparent quartz window is needed to work in established environments.

2.1.2. Residence time analysis

In the last decades, several models have been carried out to predict the residence time of particles in classical rotary kilns. Most of the authors proposed correlations based on few parameters. Usually those parameters were geometrical characteristics of the reactor or particles and a combination of some of them was normally used. Main parameters were the angle of repose of the particles, mass flow, reactor size, reactor slope, rotational speed, diameter, length, height of the dam, among others.

Normally, those correlations were based on laboratory rotary kilns whose dimensions were considerably smaller than industrial ones. Renaud et al. (2000) realized a comparative of some of these correlations with the experimental results obtained from an industrial rotary kiln. They observed most of the equations, when applied to larger reactors, underestimated the residence time from four to eight times, which means that most of the

correlations proposed were not applicable for the scale up of such devices. Hence, they suggested some improvements to the quite complex model developed by Cholette and Cloutier (1959) to predict the residence time, obtaining a good approximation with experimental results (lower than 9%). Nevertheless, one of the simplest correlation was the Sai's one which underestimated the experimental residence time less than 1.2 times. Hence, for the sake of simplicity this equation was used in the present work to estimate the residence time of a scaled up solar reactor. Sai's correlation is the following (Sai et al., 1990):

$$\tau = 60 \cdot \frac{1315.2 \cdot {h_{dam}}^{0.24}}{s^{1.02} \cdot N^{0.88} \cdot F^{0.072}} \quad (1)$$

where s is the slope of the reactor in degree, N is the reactor rotational speed in rpm, F is the mass flow in kg/h, and h_{dam} is the height of the dam in m. The dam allows maintaining the particle bed inside the reactor with an almost constant height along the axial directions to favor particle mixing and to increase the residence time.

2.1.3 Mass flow

In order to calculate the proper height of the reactor dam, a design mass flow has to be defined. Because of the characteristics of rotary kilns, the mass flow is estimated from the fill ratio (FR). As mentioned above, the fill ratio corresponds to the percentage of the reactor volume occupied by the particles. If the reactor cross section A_{RR} is assumed constant, it is possible to evaluate the area (A_p) and the height of the bed (h_{bed}) for a specific fill ratio. For a determined design conditions, the dam of the reactor has to be lower or close to the predicted bed height. In following equations, bed height was employed because it was considered the maximum limit for dam height ($h_{dam} \approx h_{bed}$). Equations 2, 3 and 4 show the formulae to evaluate the fill ratio, particle area and bed height:

$$FR = \frac{\dot{m} \cdot \tau}{V_{RR} \cdot \rho_b} \quad (2)$$

$$A_p = A_{RR} \cdot FR = \frac{1}{2} \cdot R^2 \cdot (\alpha - \sin\alpha) \quad (3)$$

$$h_{bed} = R \cdot (1 - \cos\frac{\alpha}{2}) \quad (4)$$

where $\dot{m}$ is the mass flow in kg/s, V_{RR} is the volume of the reactor, ρ_b is the bulk density of the particles, R is the radius of the reactor cross section, and α is the central angle determined by the particle bed.

Typical values for the fill ratio are limited in a range from 10 to 25% to achieve a good mixing of particles and they generally correspond to rolling and cascading subtypes of bed-motion in Mellmann classification (Mellmann, 2001). In the rolling mode, the solid material lines the bottom of the inner wall of the reactor up to a certain height and then the particles roll down on the upper surface of the bed. Thus, the particles that roll down constitute the active layer, while the particles that rotate as rigid body with the wall of the cylinder form the passive layer. From a certain fill ratio, a core of static particles appears in the central region of the bed, where mixing is not achieved. Analogously, when particles with different size or density are introduced inside the reactor, smaller and more dense particles segregate and form a static core (Boateng and Barr, 1996).

Moreover, the equation that links the absorbed power with the inlet and outlet temperatures was added to the previous ones (see equation 5). In this way, the proper residence time, the mass flow, the fill ratio and the height of the bed were calculated.

$$Q_p = \dot{m} \cdot (c_p^{T_{out}} \cdot T_{out} - c_p^{T_{in}} \cdot T_{in}) \quad (5)$$

where c_P is the specific heat of the treated material at the inlet (T_{in}) and outlet temperature (T_{out}).

2.2. Thermal Model

Heat transfer mechanisms are different in solar rotary reactor from traditional industrial kilns. In solar reactor, radiation is the main mechanism, while in classic kilns, particles heating is due to a combination of convection and radiation from the hot gas. Hence, in order to calculate the efficiency of the rotary kiln, a thermal model based on a particular cavity receiver was carried out. In the model, each kind of thermal losses was estimated following correlations found in literature. The gross power required (Q_{RR}) by the rotary receiver was calculated as the sum of the power absorbed by the particles (Q_p) and the total thermal losses (Q_l), see equation 6. In addition, kiln efficiency (η_{RR}) was obtained from equation 7.

$$Q_{RR} = Q_l + Q_p \quad (6)$$

$$\eta_{RR} = \mathrm{Q_p}/\mathrm{Q_{RR}} \quad (7)$$

Thermal losses were divided in radiative, convective, conductive, and reflection losses (see equation 8). Since conductive losses in solar receivers are more than one order of magnitude lower than other contributions, they were neglected in this work.

$$Q_l = Q_{l_{rad}} + Q_{l_{cv}} + Q_{l_{cd}} + Q_{l_{refl}} \quad (8)$$

2.2.1. Radiative losses

Radiative losses ($Q_{l_{rad}}$) were calculated with Stefan-Boltzmann law (see eq. 9) considering the effective emissivity ε_{eff} of a cylindrical cavity. In equation 9, $\sigma = 5.67 \cdot 10^{-8}$ W m^{-2} K^{-1} is the constant of Stefan-Boltzmann, A_{ap} is the aperture area of the rotary kiln, T_{amb} is the environment temperature, T_{cav} is the average temperature inside the reactor calculated with equation 10 and A_{cav} is the total area of internal surfaces of the reactor. T_i represents the average temperature of each surface that composes the cavity. In this case, the average bed temperature and the average wall temperature (T_w) were used. T_w was considered equal to stagnation temperature obtained from the average heat flux (q'') received by the internal cavity surfaces, see equation 11.

$$Q_{l_{rad}} = \varepsilon_{eff} \cdot \sigma \cdot \mathrm{A_{ap}} \cdot (T_{cav}^4 - T_{amb}^4) \quad (9)$$

$$T_{cav} = \frac{\sum_i T_i \cdot A_i}{\sum_i A_i} = \frac{\sum_i T_i \cdot A_i}{A_{cav}} \quad (10)$$

$$T_w = \sqrt[4]{\frac{q''}{\sigma \cdot \varepsilon_w}} = \sqrt[4]{\frac{Q_p}{A_{cav} \cdot \sigma \cdot \varepsilon_w}} \quad (11)$$

ε_{eff} was calculated following the methodology indicated in Bergman et al., (2011) applied to a cylindrical cavity with an aperture in one base (see equation 12). ε_{cav} corresponds to the average internal cavity emissivity, and the view factor ($F_{cav \to ap}$) was defined with equation 13. The radius of the aperture was assumed equal to the difference between the internal radius of the reactor and the dam height (see equation 15).

$$\varepsilon_{eff} = \frac{1}{F_{cav \to ap} \cdot \frac{1-\varepsilon_{cav}}{\varepsilon_{cav}} + 1} \quad (12)$$

$$F_{cav \to ap} = \frac{R_{ap}^2}{2 \cdot \mathrm{R}^2 - \mathrm{R_{ap}^2} + 2 \cdot \mathrm{R} \cdot \mathrm{L}} \quad (13)$$

$$A_{ap} = \pi \cdot \mathrm{D_{ap}^2}/4 \quad (14)$$

$$D_{ap} = 2 \cdot \mathrm{R_{ap}} = 2 \cdot (R - \mathrm{h_{dam}}) \quad (15)$$

2.2.2. Convective losses

In case of an open cavity rotary kiln, convective losses $Q_{l_{cv}}$ were expected similar to the losses of a static solar cavity receiver. Because rotational speed were not high and it was supposed the reactor/receiver was protected by a well-insulated static case, losses from the external walls of the reactor were neglected. Otherwise, convective losses in the interior of the cavity are not easy to calculate and a specific study has to be done on a case by case basis. However, several correlations have been proposed and used by many authors (Li et al., 2010; Ma, 1993; Mcdonald, 1995; Siebers and Kraabel, 1984). In this work, the methodology proposed by Siebers and Kraabel (1984) was followed. Convection losses were separated in forced $Q_{l_{cv}}^f$ and natural $Q_{l_{cv}}^n$ contributions as indicated in equation 16 and 17. Where *Nu* is the number of Nusselt, *K* the conductivity of the air and *D* the diameter of the reactor.

$$Q_{l_{cv}} = Q_{l_{cv}}^f + Q_{l_{cv}}^n = h_{conv} \cdot (T_{cav} - T_{amb}) \cdot A_{cav} \quad (16)$$

$$h_{conv} = h_{nc} + h_{fc} = \frac{Nu_{nc} \cdot K}{D} + \frac{Nu_{fc} \cdot K}{D} \quad (17)$$

Stine and Mcdonald indicated *Nu* for natural convection can be calculated by equations 18, 19 and 20, where *Gr* is the number of Grashof ($10^5 < \mathrm{Gr} < 10^{12}$); β, the coefficient of volumetric expansion; ν, the cinematic viscosity of the air at the ambient temperature, and *g* is the gravity acceleration (Mcdonald, 1995).

$$Nu_{nc} = 0.088 \cdot Gr^{\frac{1}{3}} \cdot \left(\frac{T_{cav}}{T_{amb}}\right)^{0.18} \cdot (\cos s)^{2.47} \cdot \left(\frac{Dap}{D}\right)^{S} \quad (18)$$

$$Gr = \frac{g \cdot \beta \cdot (T_{cav} - T_{amb}) \cdot D^3}{\nu^2} \quad (19)$$

$$S = 1.12 - 0.982 \cdot \left(\frac{D_{ap}}{D}\right) \quad (20)$$

To calculate *Nu* for forced convection, the following correlation from Ma (1993) was used:

$$h_{fc} = 0.1967 \cdot v_{wind}^{1.849} \quad (21)$$

where v_{wind} is the wind speed.

For the treatment of reactive particles or direct treatment of materials, a controlled atmosphere inside the reactor is required. Therefore, a window at the kiln aperture must be employed. In these cases, similar to industrial rotary kilns, convective heat losses are mainly due to the forced fluid flow inside the reactor. Nevertheless, gases in solar kilns are at relatively low temperatures and the heat passes from the wall and particles to the gas. On the contrary, in industrial devices, the heat passes from the hot gas to the particles and to the kiln walls. For this configuration, no specific equations have been developed so far, neither for solar rotary kilns nor for industrial rotary kilns. For instance, Brimacombe and Watkinson correlation underestimated convective heat losses for their classical rotary kiln (Brimacombe and Watkinson, 1978; Watkinson and Brimacombe, 1978). Yang and Farouk correlation was also discarded for the same reason (Yang and Farouk, 1997).

2.2.3. Reflection losses

In solar plants, part of the radiation impinging on the receiver is reflected by the receiver surface towards the environment. Cavity receivers reduce these losses, which can be calculated with equation 22. ρ_{cav} is the reflectivity of the internal surfaces of the cavity and it is calculated through equation 23 as the weight average reflectivity for the different constituent materials.

$$Q_{l_{refl}} = F_{cav \to ap} \cdot \rho_{cav} \cdot Q_{RR} \quad (22)$$

$$\rho_{cav} = \frac{(1-\varepsilon_w) \cdot A_w + (1-\varepsilon_p) \cdot A_{bed}}{A_{cav}} \quad (23)$$

2.3. Heliostats fields design

Solar tower plants consist of a receiver mounted on the top of a tower and a heliostat field. The distribution of the heliostat field can be either circular (around the tower), or at one side of the tower (north or south field, depending on the hemisphere where the plant is located). Because solar rotary kiln shape is similar to cavity receiver, only one-side configuration is suitable for these thermal processes. For this reason, the power range of such a solar tower plant is limited to 1-100 MWth, approximately.

In order to define the heliostat field for the plant, the software WinDelsol was used. WinDelsol is based on the original Delsol3 code from SANDIA National Labs. The software can design and optimize heliostat fields and determine the radiative flux on cavity, external or flat receivers. In this case, a tilted flat receiver was employed in order to reproduce the flux that reaches the aperture of the reactor. The location of the plant was supposed in the Tabernas Desert, Almeria (Spain) for which atmospheric attenuation parameters were known. Detailed characteristics of heliostats, aiming strategies and the required power on the receiver were introduced in the software as inputs for the calculation. With this information, WinDelsol could estimate the flux distribution on the selected receiver and at the same time, it delivered the optimized heliostat field, considering thermal losses due to cosine factor, shadowing, blocking, spillage and atmospheric attenuation. WinDelsol delivered also the number of heliostats (N_{HS}), the efficiency (η_{HS}), the total area ($N_{HS} \cdot A_{HS}$) and the reflected power (Q_{HS}) by the heliostat field. Alternatively, knowing the number of heliostats and the reference direct normal irradiation (DNI_{ref}), the power reflected by the heliostat field could be obtained with equation 24 and the efficiency with 25. A_{HS} is the reflecting surface of one heliostat. In this study, a minimum efficiency of 70% for the heliostat field was considered acceptable.

$$\mathrm{Q_{HS}} = N_{HS} \cdot A_{HS} \cdot DNI_{ref} \quad (24)$$

$$\eta_{HS} = \mathrm{Q_{RR}}/\mathrm{Q_{HS}} \quad (25)$$

Finally, the total efficiency of the plant can be calculated with equation 26.

$$\eta_{tot} = \mathrm{Q_p}/\mathrm{Q_{HS}} = \eta_{HS} \cdot \eta_{RR} \quad (26)$$

2.4. Storage system considerations

In this work, the kiln was treated as a thermal rotary receiver for sand or particles. Depending on the requirements, the system can store or not the absorbed solar energy. As previously explained, the shape of the reactor limits the maximum power available and, when the thermal demand is high, a plant without storage could result more advantageous to produce hot air, water or steam in a heat exchanger with the integration of an auxiliary heater. In other cases, when the heat demand of the process is considerably lower than the maximum power of the solar plant, a storage system should be considered. Thus, a specific solar multiple has to be defined for the plant, taking into account the requirements of each case. Finally, in plants working with direct treatment of material, a batch reactor could be more appropriate than a continuous one.

As mentioned, the plant can operate with or without thermal storage. If the plant is provided with an insulated hot tank, when the heat demand decreases or is null, the sand can be stored in it. In this way, the control of sand energy could be easier. However, residence time could not be sufficient to heat up the sand because of the intermittency and variations of solar energy. Although residence time can be varied by changing the rotational speed of the reactor, recirculation of sand in the reactor or an auxiliary heating system inside the hot storage should be implemented in order to achieve the desired particle temperature when weather conditions are not ideal. A schematic representation of a plant with thermal storage and with direct treatment of material is shown in figure 1.

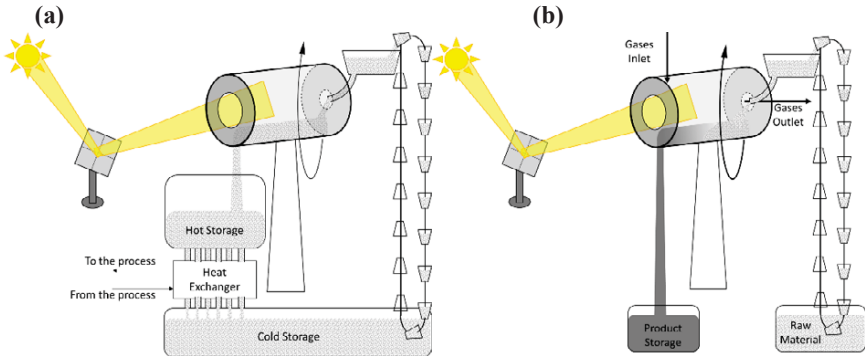

Fig. 1: Configurations of a plant a) with thermal storage and b) for direct treatment of material in the receiver.

3. Results

3.1. Receiver sizing, residence time and mass flow

A reference case based on PS10 solar tower plant is presented for which a thermal power (Q_p) of 50 MW was considered. Kiln size was determined in order to be similar to PS10 receiver. Furthermore, a rotational speed of 5 rpm and a receiver slope of 5° were assumed. Those values are within the typical range for industrial rotary kilns and they assure a bed motion in rolling or cascading mode. As mentioned, sand was the material designated for the study with a design outlet temperature of 750 °C. The considered sand properties were bulk density (1560 kg/m^3) and the specific heat, which was calculated at the entrance and at the outlet of the reactor according to equations 27 and 28 (Perry, 1997). In the case of a plant without storage, in which the particles are directly irradiated, the specific heat of sand has to be changed with the treated material's one (this case is not reported here). Sand properties used in the calculation are resumed in table 1.

$$C_{p_{SiO2,\alpha}} = \frac{4.187}{0.06} \cdot \left(10.87 + 0.008712 \cdot T - \frac{241200}{T^2}\right) \quad \text{for } 273 < T < 848 \text{ K} \quad (27)$$

$$C_{p_{SiO2,\beta}} = \frac{4.187}{0.06} \cdot (10.95 + 0.0055 \cdot T) \quad \text{for } 848 < T < 1873 \text{ K} \quad (28)$$

Table 1: Main physical properties of sand used for calculations.

Property	bulk density	Specific heat at 20 °C	Specific heat at 750 °C
Unit	kg/m^3	J kg^{-1} K^{-1}	J kg^{-1} K^{-1}
Sand	1560	740.9	1156.8

An iterative process was adopted in order to determine the proper size of the receiver. According to Mellmann classification, a fill ratio higher than 10% assures the achievement of a rolling bed motion inside the kiln. Nevertheless, increasing the fill ratio, segregation can arise inside the core of the particle bed. Another constraint is related to kiln aperture. As indicated above, aperture diameter depends on the height of the particle bed that defines the height of the kiln dam. A small aperture can reduce receiver heat losses; however, if it is too small, part of the flux reflected by the heliostat field could not enter and, as a consequence, spillage losses increase. Taking into account this consideration, an internal diameter of 9 m and an axial length of 8.7 m were selected for the receiver.

Table 2: Rotary kiln geometrical and operational characteristics.

Parameter	Internal Diameter	Length	Dam Height	Aperture Diameter	Fill Ratio	Residence Time	Mass Flow	Central Angle α
Unit	m	m	m	m	%	min	kg/s	degree
Value	9	8.7	1.4	6.2	10	28	51.7	93.3

3.2. Thermal model results

For the calculations, it was assumed that the rotary kiln had been heated before the addition of the particles. Once the size of the receiver was fixed and mass flow and temperature range were known, thermal losses were calculated. Air parameters used in the equations are shown in table 3. To evaluate radiative losses, a wall and a particle emissivity of 0.8 (Zhou et al., 2006) and 0.76 ("Engineering Toolbox," 2016) respectively, were assumed.

Table 3: Main physical properties of air used for calculations.

Property	Cinematic viscosity	Volumetric expansion	Conductivity	Wind speed
Symbol	ν	β	K	v
Unit	m^2/s	1/K	W m^{-1} K^{-1}	m/s
Air	$15.11 \cdot 10^{-6}$	$3.43 \cdot 10^{-3}$	0.0515	10

With these values, the results shown in table 4 were obtained. In case 1, convective losses were calculated considering an open cavity receiver, following the methodology proposed by Siebers and Kraabal with the correlation of Stine and Mcdonald for the natural convection and Ma´s correlation for the forced convection.

Table 4: Thermal results for the rotary kiln without transparent windows at the aperture.

	Inlet temp.	Outlet temp.	Absorbed Power	Radiative Losses	Convective Losses	Reflection Losses	Efficiency
Unit	°C	°C	MW	MW	MW	MW	%
Value	750	20	50	3.42	5.45	1.12	83

3.3. Heliostat field results

Two heliostat fields were calculated, assuming Tabernas Desert conditions, a tower height of 110 m and a minimum efficiency of 70%. The first field was based on PS10 heliostats. Those mirrors had a large size and a reflecting surface of 121 m^2 each one. Field with larger heliostats had the advantage to be cheaper, mainly because a minor number of elements is needed. With 713 heliostats, it was possible to concentrate 60 MW of solar radiation inside a circular area of 8 m in diameter placed at the receiver aperture plane. A maximum flux of 2320 kW/m^2 and an average flux of 994 kW/m^2 at the aperture were predicted. A secondary concentrator at the entrance of the kiln was needed because the calculated aperture of the kiln was smaller than the achieved flux distribution. Moreover, a second heliostat field was designed, considering a smaller heliostat size (13.5 m^2). In this case, it was predicted a heliostat field of 6622 elements, a maximum heat flux of 3620 kW/m^2 and an average one of

1656 kW/m^2. For this case, the flux fitted inside the kiln aperture of 6.2 m. In Fig. 2 both heliostat fields are shown.

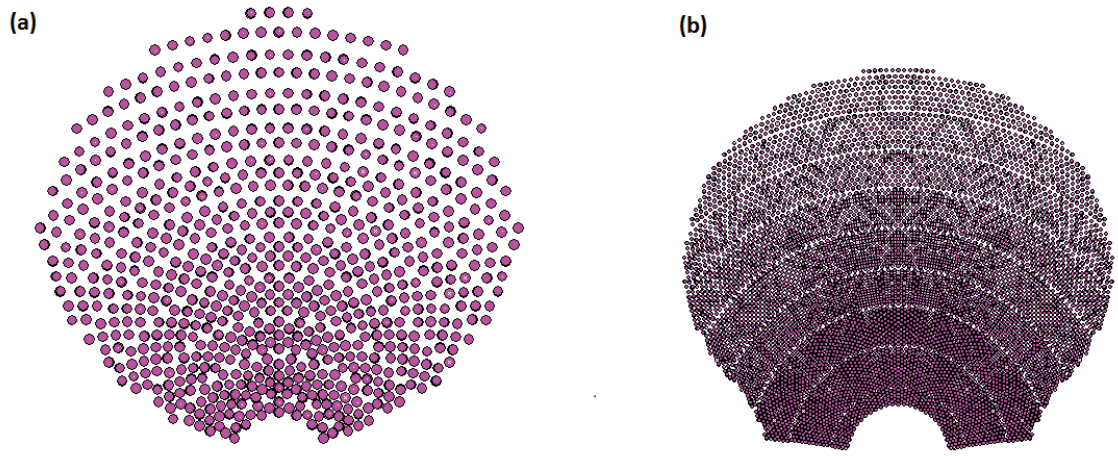

Fig. 2: Heliostat field a) with large heliostats and b) with small heliostats.

4. Discussion and further considerations

The design of the rotary receiver required the selection of several parameters. Geometrical parameter were based on the existing PS10 tower plant and solar rotary kilns proposed so far. In the analyzed example, the mass flow through the kiln was determined by the design power of the receiver and temperature conditions at the inlet and outlet. Working with solid particles at ambient temperature avoids freezing problems of conventional thermal fluids and reduces storage costs in comparison with other heat transfer fluids (i.e., molten salts). Moreover, because of the wider working temperature range, lower mass flows are needed to obtain an equal absorbed power. The outlet temperature of 750 °C was selected because it was higher than the limit of current commercial heat transfer fluid, but it was low enough to avoid a considerable increase of material cost, in particular, the cost of the transport system of the particles, heat exchanger and hot storage tank. Moreover, working with higher temperatures implies reducing the mass flow and as consequence the fill ratio or the kiln aperture. For the proposed example, those parameters were close to their lower limits.

Residence time estimation are quite complex for rotary kilns and in most cases, they are not applicable for scaling up from lab devices. Residence time presented in this work is a rough evaluation of the experimental residence time of an industrial rotary kiln. In the future, a detailed model for the rotary kiln will be developed with the aim to achieve more reliable results and to improve the scale up of such a device. Nevertheless, the estimation of the residence time presented in this work could be assumed as an initial information for the scale up of the plant. A calculated time of 28 min is a reasonable time for the operation in a solar device. An important issue for this solar systems is the control of particle temperature and because of variation in weather conditions, higher residence time could make it complex.

For the thermal model, the rotary kiln was considered similar to a cavity receiver and calculations were based on the existing models for this kind of elements. Therefore, calculated efficiency resulted close to typical efficiencies of these receivers. One of the greatest challenges for both, cavity receivers and rotary kilns, is a good prediction of convective losses. Moreover, an important difference consists in the heat transfer mechanisms for those technologies. In particular, for cavity receivers and solar rotary kilns, radiation is the principal mechanism, while for rotary kilns a combination of convection and radiation from the gas to the solid particles and the walls is the main one. In this work, a simplified model for convective losses was used for the case of a rotary receiver with an open aperture. The proposed thermal model indicates convective losses are the most relevant, corresponding to more than 5 MW. Radiative and reflective losses are 3.42 and 1.12 MW, respectively.

Heliostat fields obtained with the software WinDelsol present higher fluxes than those used in solar tower plants for electricity production. However, they are in an acceptable range for this kind of technology. For both heliostat fields the efficiency was 70% and, as it can be seen in figure 2, a more compact field can be obtained if smaller heliostats are used. Second field allows to fit the flux inside the reactor aperture without the need of a second concentrator. As a drawback, a considerable higher number of heliostats is needed and that could increase the

cost of the plant.

As future work, studies on a solar rotary kiln, which operates in batch mode, will be carried on. This operational mode could facilitate control of the temperature inside the receiver/reactor, but it needs time for charge and discharge phases. As a consequence, during these phases, part of the daily solar radiation cannot be used.

5. Conclusions

Considerations on central receiver plants with rotary kiln for production of process heat with or without storage have been analyzed and discussed in this work. In particular, the case of a 50 MW_{th} plant is presented. Because of the shape of rotary kilns, only one-side heliostat field can be suited in this kind of solar tower plant. A rotary kiln with sand particles is analyzed. A simplified thermal model was carried on and a receiver efficiency of 83% was calculated. A sand residence time of 28 minutes was also predicted. Finally, two heliostat fields are proposed. The first one consists of 713 large heliostats which focus solar energy on a secondary concentrator of 8 m in diameter. With the second one, it is possible to concentrate the required power by the receiver on the aperture of the kiln without the use of a secondary concentrator. As a drawback, more than 6600 small heliostats are needed. To conclude, a first analysis of central tower plants with rotary receiver was conducted. Initial results show the possibility to realize solar plants with these characteristics in future developments. However, more detailed models must be studied in order to more accurately predict the performance of such systems.

Acknowledgments

The authors acknowledge the financial support provided by the FONDECYT project number 3150026 of CONICYT (Chile), the Education Ministry of Chile Grant PMI ANT 1201, and the Solar Energy Research Center SERC Chile. The second author also wish to thank the University of Almeria and the Plataforma Solar de Almería for the assistance and collaboration devoted to the development of his Ph.D research.

6. References

Alonso, E., Pérez-Rábago, C.A., Licurgo, J., Fuentealba, E., Estrada, C.A., 2015. First experimental studies of solar redox reactions of copper oxides for thermochemical energy storage. Sol. Energy 115, 297–305. doi:10.1016/j.solener.2015.03.005

Alonso, E., Romero, M., 2015. Review of experimental investigation on directly irradiated particles solar reactors. Renew. Sustain. Energy Rev. 41, 53–67. doi:10.1016/j.rser.2014.08.027

Aydin, D., Casey, S.P., Riffat, S., 2015. The latest advancements on thermochemical heat storage systems. Renew. Sustain. Energy Rev. 41, 356–367. doi:10.1016/j.rser.2014.08.054

Bergman, T.L., Incropera, F.P., DeWitt, D.P., Lavine, A.S., 2011. Fundamentals of Heat and Mass Transfer.

Block, T., Schmücker, M., 2016. Metal oxides for thermochemical energy storage: A comparison of several metal oxide systems. Sol. Energy 126, 195–207. doi:10.1016/j.solener.2015.12.032

Boateng, A.A., Barr, P. V., 1996. Modelling of particle mixing and segregation in the transverse plane of a rotary kiln. Chem. Eng. Sci. 51, 4167–4181. doi:10.1016/0009-2509(96)00250-3

Brimacombe, J.K., Watkinson, A.P., 1978. Heat transfer in a direct-fired rotary kiln: I. Pilot plant and experimentation. Metall. Trans. B 9, 201–208. doi:10.1007/BF02653685

Calderoni, M., Aprile, M., Moretta, S., Aidonis, A., Motta, M., 2012. Solar thermal plants for industrial process heat in Tunisia : Economic feasibility analysis and ideas for a new policy 30, 1390–1400. doi:10.1016/j.egypro.2012.11.153

Cholette, A., Cloutier, L., 1959. Mixing efficiency determinations for continuous flow systems. Can. J. Chem. Eng. 37, 105–112. doi:10.1002/cjce.5450370305

Engineering Toolbox [WWW Document], 2016. URL http://www.engineeringtoolbox.com/emissivity-coefficients-d_447.html (accessed 10.6.16).

Fuller, R.J., 2011. Solar industrial process heating in Australia - Past and current status. Renew. Energy 36, 216–221. doi:10.1016/j.renene.2010.06.023

Gallo, A., Spelling, J., Romero, M., González-Aguilar, J., 2015. Preliminary Design and Performance Analysis of a Multi-Megawatt Scale Dense Particle Suspension Receiver. Energy Procedia 0, 388–397. doi:10.1016/j.egypro.2015.03.045

Halmann, M., Steinfeld, A., Epstein, M., Guglielmini, E., Vishnevetsky, I., 2012. Vacuum Carbothermic Reduction of Alumina, in: proceedings of ECOS 2012 - the 25th international conference on efficiency, cost, optimization, simulation and environmental impact of energy systems.

Jemmal, Y., Zari, N., Maaroufi, M., 2016. Thermophysical and chemical analysis of gneiss rock as low cost candidate material for thermal energy storage in concentrated solar power plants. Sol. Energy Mater. Sol. Cells 157, 377–382. doi:10.1016/j.solmat.2016.06.002

Kousksou, T., Bruel, P., Jamil, a., El Rhafiki, T., Zeraouli, Y., 2014. Energy storage: Applications and challenges. Sol. Energy Mater. Sol. Cells 120, 59–80. doi:10.1016/j.solmat.2013.08.015

Lauterbach, C., Schmitt, B., Jordan, U., Vajen, K., 2012. The potential of solar heat for industrial processes in Germany. Renew. Sustain. Energy Rev. 16, 5121–5130. doi:10.1016/j.rser.2012.04.032

Li, X., Kong, W., Wang, Z., Chang, C., Bai, F., 2010. Thermal model and thermodynamic performance of molten salt cavity receiver. Renew. Energy 35, 981–988. doi:10.1016/j.renene.2009.11.017

Liu, M., Steven Tay, N.H., Bell, S., Belusko, M., Jacob, R., Will, G., Saman, W., Bruno, F., 2016. Review on concentrating solar power plants and new developments in high temperature thermal energy storage technologies. Renew. Sustain. Energy Rev. 53, 1411–1432. doi:10.1016/j.rser.2015.09.026

Ma, R.Y., 1993. Wind Effects on Convective Heat Loss From a Cavity Receiver for a Parabolic Concentrating Solar Collector.

Mahlia, T.M.I., Saktisahdan, T.J., Jannifar, A., Hasan, M.H., Matseelar, H.S.C., 2014. A review of available methods and development on energy storage ; technology update. Renew. Sustain. Energy Rev. 33, 532–545. doi:10.1016/j.rser.2014.01.068

Mcdonald, C.G., 1995. Heat Loss from an Open Cavity.

Meier, A., Bonaldi, E., Cella, G.M., Lipinski, W., Wuillemin, D., Palumbo, R., 2004. Design and experimental investigation of a horizontal rotary reactor for the solar thermal production of lime. Energy 29, 811–821. doi:10.1016/S0360-5442(03)00187-7

Mellmann, J., 2001. The transverse motion of solids in rotating cylinders—forms of motion and transition behavior. Powder Technol. 118, 251–270. doi:10.1016/S0032-5910(00)00402-2

Nikulshina, V., Gebald, C., Steinfeld, a., 2009. CO2 capture from atmospheric air via consecutive CaO-carbonation and CaCO3-calcination cycles in a fluidized-bed solar reactor. Chem. Eng. J. 146, 244–248. doi:10.1016/j.cej.2008.06.005

Pardo, P., Deydier, A., Anxionnaz-Minvielle, Z., Rougé, S., Cabassud, M., Cognet, P., 2014. A review on high temperature thermochemical heat energy storage. Renew. Sustain. Energy Rev. 32, 591–610. doi:10.1016/j.rser.2013.12.014

Perry, R.H., 1997. Perry's Chemical Engineers' Handbook, 7th ed. McGraw-Hill, New York.

Renaud, M., Thibault, J., Trusiak, A., 2000. Solids Transportation Model of an Industrial Rotary Dryer. Dry. Technol. 18, 843–865. doi:10.1080/07373930008917741

Romero, M., Steinfeld, A., 2012. Concentrating solar thermal power and thermochemical fuels. Energy Environ. Sci. 5, 9234. doi:10.1039/c2ee21275g

Sai, P.S.T., Surender, G.D., Damodaran, A.D., Suresh, V., Philip, Z.G., Sankaran, K., 1990. Residence time distribution and material flow studies in a rotary kiln. Metall. Mater. 21, 1005–1011. doi:10.1007/BF02670271

Siebers, D.L., Kraabel, J.S., 1984. Estimating Convective Energy Losses From Solar Central Receivers. SANDIA Rep.

Steinfeld, A., 2005. Solar thermochemical production of hydrogen—a review. Sol. Energy 78, 603–615. doi:10.1016/j.solener.2003.12.012

Watkinson, A.P., Brimacombe, J.K., 1978. Heat transfer in a direct-fired rotary kiln: II. Heat flow results and their interpretation. Metall. Trans. B 9, 209–219. doi:10.1007/BF02653686

Yang, L., Farouk, B., 1997. Modeling of Solid Particle Flow and Heat Transfer in Rotary Kiln Calciners. J. Air Waste Manage. Assoc. 47, 1189–1196. doi:10.1080/10473289.1997.10464069

Zhang, H., Benoit, H., Gauthier, D., Degrève, J., Baeyens, J., López, I.P., Hemati, M., Flamant, G., 2016. Particle circulation loops in solar energy capture and storage: Gas–solid flow and heat transfer considerations. Appl. Energy 161, 206–224. doi:10.1016/j.apenergy.2015.10.005

Zhou, B., Yang, Y., Reuter, M.A., Boin, U.M.J., 2006. Modelling of aluminium scrap melting in a rotary furnace. Miner. Eng. 19, 299–308. doi:10.1016/j.mineng.2005.07.017